

Alternative Splicing Modulates Inactivation of Type 1 Voltage-gated Sodium Channels by Toggling an Amino Acid in the First S3-S4 Linker*

Received for publication, April 12, 2011, and in revised form, September 1, 2011. Published, JBC Papers in Press, September 2, 2011, DOI 10.1074/jbc.M111.250225

Emily V. Fletcher¹, Dimitri M. Kullmann², and Stephanie Schorge³

From the Department of Clinical and Experimental Epilepsy, UCL Institute of Neurology, London WC1N 3BG, United Kingdom

Background: Small changes in voltage-gated sodium channel behavior can disrupt neuronal activity and cause severe neurological disorders.

Results: By changing a single amino acid, a conserved alternative splicing event modifies the stability of channel inactivation.

Conclusion: Splicing can regulate inactivation of sodium channels.

Significance: Many commonly used drugs target sodium channel inactivation; consequently, splicing could affect treatment of several neurological disorders.

Voltage-gated sodium channels underlie the upstroke of action potentials and are fundamental to neuronal excitability. Small changes in the behavior of these channels are sufficient to change neuronal firing and trigger seizures. These channels are subject to highly conserved alternative splicing, affecting the short linker between the third transmembrane segment (S3) and the voltage sensor (S4) in their first domain. The biophysical consequences of this alternative splicing are incompletely understood. Here we focus on type 1 sodium channels (Nav1.1) that are implicated in human epilepsy. We show that the functional consequences of alternative splicing are highly sensitive to recording conditions, including the identity of the major intracellular anion and the recording temperature. In particular, the inactivation kinetics of channels containing the alternate exon 5N are more sensitive to intracellular fluoride ions and to changing temperature than channels containing exon 5A. Moreover, Nav1.1 channels containing exon 5N recover from inactivation more rapidly at physiological temperatures. Three amino acids differ between exons 5A and 5N. However, the changes in sensitivity and stability of inactivation were reproduced by a single conserved change from aspartate to asparagine in channels containing exon 5A, which was sufficient to make them behave like channels containing the complete exon 5N sequence. These data suggest that splicing at this site can modify the inactivation of sodium channels and reveal a possible interaction between splicing and anti-epileptic drugs that stabilize sodium channel inactivation.

Alternative splicing is highly conserved in vertebrate voltage-gated sodium channels (1, 2), suggesting that it plays an impor-

tant role in modulating channel function. Because sodium channels underlie neuronal excitability (3) and mutations that induce small changes in their function can lead to disease, including epilepsy (4–6), there is growing interest in the functional consequences of splicing. Nav1.1 channels encoded by *SCN1A* are strongly associated with Mendelian epilepsy in humans (OMIM 182389) and are disproportionately important for interneuronal excitability (7–9).

All tetrodotoxin-sensitive neuronal sodium channels have a duplication of the exon encoding the voltage sensor (S4) in their first domain (Fig. 1). Compared with other channels, Nav1.1 has accumulated multiple evolutionary changes in one copy of this exon. Rodents have several stop codons in the “neonatal” variant, exon 5N, as well as a disrupted splice site (2), so the rodent *SCN1A* transcript including 5N does not give rise to a channel subunit, unlike the transcript containing the “adult” variant, exon 5A. Humans still have a functional copy of exon 5N but have acquired several amino acid changes in the coding sequence as well as a splice site polymorphism that reduces expression of the exon (10, 11). The genotype of this splice site polymorphism is associated with altered dosage of several front line anti-epileptic drugs (11, 12), suggesting that altered splicing in *SCN1A* may modify drug responsiveness. However, this finding has not been replicated in one study (13). The polymorphism and potentially alternative splicing at this site in *SCN1A* has also been associated with an increased likelihood of carbamazepine resistance in epilepsy (14) or with febrile seizures (15). Again, the status of these associations is uncertain because the former study was small and the latter was not replicated in a different population (16).

Although several studies have focused on the clinical and therapeutic genetic associations, which remain to be clarified, the fundamental biophysical differences between the human Nav1.1 splice variants are unknown. Several groups have investigated the properties of splice variants of other Nav1 subunits (17–24), but no data are available for Nav1.1. This leaves the potential mechanisms linking splicing to seizure susceptibility or treatment unknown. Additionally, because this channel is known to be sensitive to modulation

* This work was supported by Medical Research Council Grant G0601440 and by the European Union (Epicure, Grant LSH 037315).

⌘ Author's Choice—Final version full access.

¹ Supported by a Brain Research Trust studentship.

² Funded by the Medical Research Council, the Wellcome Trust, and the European Research Council.

³ Funded by a fellowship by the Worshipful Company of Pewterers. To whom correspondence should be addressed: DCEE 8th floor QSH, UCL-Institute of Neurology Queen Square, London WC1N 3BG. E-mail: s.schorge@ion.ucl.ac.uk.

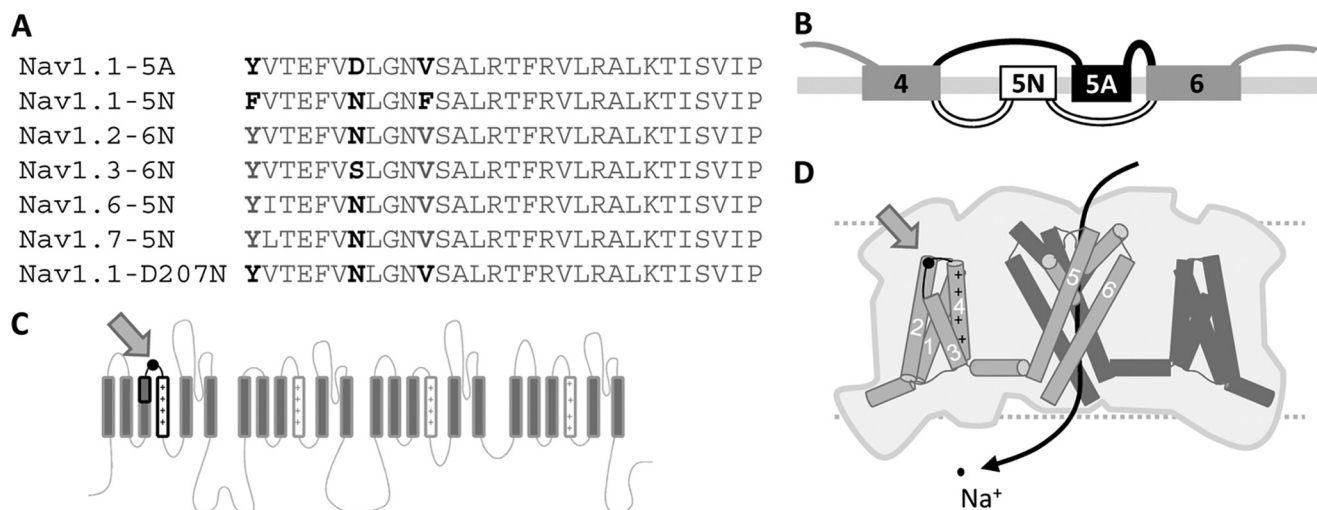


FIGURE 1. Structure and conservation of splicing in voltage-gated sodium channels. *A*, conservation of the alternate N exon in neuronal sodium channels is shown. All sequences are human and correspond to the short extracellular S3-S4 linker and the S4 voltage sensor in domain I. The sequence for Nav1.1 corresponds to amino acids 201–230 of the mature peptide, which is determined by this exon. Nav1.1-D207N is identical to Nav1.1-5A except for the Asp → Asn substitution, which is conserved in Nav1.1, -1.2, -1.6, and -1.7. In Nav1.2 and -1.3 the homologous splicing region is designated as exon 6 due to different exon numbering in the consensus gene sequence but represents the region homologous to that encoded by exon 5 in the other genes. *B*, shown is the genomic structure of human *SCN1A* in the region of exons 5A and 5N (6A and 6N in *SCN2A* and *SCN3A*). The A and N exons are each 92 nucleotides long and are exclusive. Inclusion of both or neither of the exons would lead to a frameshift. *C*, shown is a schematic of the predicted topology of Nav1.1 indicating the region encoded by exon 5N or 5A in the first domain of the channel. This region, corresponding to the end of the third transmembrane segment (S3), a short extracellular linker, and the entire voltage-sensing fourth transmembrane segment (S4) is indicated in a *black outline*. The *circle* indicated by the *arrow* is the position of the conserved D207N change imposed by splicing. *D*, shown is the proposed structure of a bacterial voltage-gated sodium channel, indicating the approximate position of the D207N substitution in the S3-S4 segment of the voltage sensing module (*arrow, black circle*). The structure is based on the recently published bacterial voltage-gated sodium channel NavAb (adapted from Fig. 1 and supplemental Fig. S6 in Payandeh *et al.* (43)). The pale *gray cylinders* and linkers represent one domain of the channel (domain I). The *darker cylinders* indicate the position of the opposite domain (III), and the outline is the proposed space-filling shape of the protein, with *dotted lines* indicating the thickness of the plasma membrane. Domains II and IV are not shown.

by G-proteins (25) and temperature sensitivity is a hallmark of diseases associated with it (4–6), it is important to investigate the properties of splice variants in conditions that allow for G-protein modulation under near-physiological conditions.

Our goal was to determine if splicing has a consistent effect on any of the intrinsic parameters of Nav1.1 function. We show that the splice variants exhibit differences in inactivation kinetics and that inactivation of exon 5N-containing channels is more sensitive to recording temperature and intracellular fluoride than exon 5A-containing channels. We also identify a single amino acid that differs between the variants that is sufficient to account for the effect of alternate splicing on the rate of recovery from inactivation. These results reveal unexpected functional consequences of highly conserved alternate splicing in neuronal sodium channels.

EXPERIMENTAL PROCEDURES

Mutagenesis and Cloning of Sodium Channel Subunits—The three amino acid differences encoded by exon 5N and D207N were introduced into the human *SCN1A* cDNA (a gift of J. J. Clare) in the pcDM8 vector (gift of M. Mantegazza) using site-directed mutagenesis using the QuikChange kit according to directions (Stratagene, CA). 5N primers were CATTACATTGCGTTCGTCACAGAGTTTGTGAACCTGGGCAATTTCTCGGCATTGAG (forward) and CGAGAAATTGCCAGGTTCAAACTCTGTGACGAACGCAAATGTAATGACAGTG (reverse), and D207N were CAGAGTTTGTGAACCTGGGCAATGTCTC (forward) and ACATTGCCAGGTTCAAACTCTGTGAC(reverse).

Transformants were confirmed with sequencing. Exon 5 splice variants were characterized in a shortened version of exon 11, Nav1.1 (26), as this is thought to be the most abundant transcript in the rat brain (27).

SCN1B-ECMV^Δ IRES-SCN2B-polio IRES-EGFP, with full plasmid details in Cox *et al.* (28), was a gift from J Wood, UCL. To introduce a stop codon, three nucleotides upstream of the *SCN2B* ATG codon the following mutagenesis reaction was performed. Primers from 5' to 3' sequence were GAAAAACACGATGATAATTAGGCCACAACCATGCACAG (forward) and CTGTGCATGGTTGTGGCCTAATTATCATCGTGTTTTTC (reverse). *SCN1B* splice variant B was first cloned into the pCMV6-XL5 mammalian expression vector (Origene Technologies). This clone was used as a template to amplify *SCN1BB* with 5'-XhoI and 3'-BamHI restriction sites for subcloning into the *SCN1B-ECMV IRES-SCN2B-polio IRES-EGFP* vector. *SCN1BB* Primers from 5' to 3' sequence were ACGctcgg-CACCATGGGGAGGCTGCTGGCC (forward) and CGC-ggatccTCAAACCACACCCCGAGA (reverse). Lower case indicates introduced restriction sites.

SCN1B within SCN1B-ECMV IRES-SCN2B-polio IRES-EGFP was excised using XhoI and HindIII and replaced with *SCN1BB* using the same enzymes. All constructs were routinely sequenced after plasmid purification. Details are available upon request.

Expression—HEK293T cells (ATCC) were transfected with lipofectamine2000 (Invitrogen) according to manufacturer's

⁴ The abbreviations used are: ECMV, encephalomyocarditis virus; IRES, internal ribosome entry site; GTP-γS, guanosine 5'-3-O-(thio)triphosphate; ANOVA, analysis of variance; EGFP, enhanced green fluorescent protein.

Splicing Modifies Inactivation of Nav1.1 Channels

protocols. Recordings were carried out 48–72 h after transfection. Recordings from control cells that were not transfected did not produce detectable sodium currents (data not shown).

Electrophysiology—Recording solutions were: external, 145 mM NaCl, 4 mM KCl, 1.8 mM CaCl₂, 1 mM MgCl₂, 10 mM HEPES, pH 7.35; internal, 150 mM CsCl, 10 mM EGTA, 10 mM HEPES, pH 7.35. Where CsF was used, it replaced 140 mM CsCl in the intracellular solution. Where GTPγS was included in the intracellular solution, it was used at a final concentration of 0.5 mM. In control experiments, GTPγS did not induce currents in the absence of the Nav1.1 subunits (data not shown).

The calculated junction potentials were: CsCl = −4.4 mV; CsF = −9.3 mV. These were not corrected. Electrodes were 1–3 megaohms in resistance. Series resistance was always below 5 megaohms, generally below 2 megaohms, and was routinely compensated 50–70% in room temperature recordings only. To control for cell to cell variability, we transfected and recorded both splice variants on the same days and combined individual cells from at least three recording sessions.

All currents were recorded using a Multiclamp 700B amplifier (Molecular Devices). Data were leak-subtracted with a $-P/4$ protocol, filtered at 10 kHz, and sampled at 50 kHz. Acquisition and analysis were performed using custom programs in Labview 8.0 (National Instruments). To assess channel activation, cells were held at −80 mV and stepped to voltages between −60 and +30 mV in 10-mV intervals. Cells were allowed to recover at least 4 s between depolarizing steps. $G_{Na}/G_{Na_{max}} = 1/(1 + \exp((V_{50} - V)/k))$, where $G_{Na}/G_{Na_{max}}$ is the normalized conductance value, V_{50} is the voltage that produces half-maximal conductance, and k is the slope factor. Inactivation was fit with a mono-exponential decay after steps from −20 to +20 mV from 90% of peak current amplitude.

To calculate steady-state inactivation, channels were activated by 100-ms prepulses (−100 to −10 mV, holding potential −80 mV) followed by a 30-ms test pulse to −10 mV. Steady-state inactivation was normalized to peak current and fit in Graphpad Prism 5 with a Boltzmann function, $I_{Na} = (A + (B - A))/(1 + \exp((V_{50} - V)/k))$, where I_{Na} is the fraction of sodium current available, A is the lowest value, and B is the highest value (with V_{50} and k as above). Persistent current was calculated as the mean current from the last 10 ms of the test pulse from −80 mV and expressed as a fraction of the peak transient current.

Recovery from inactivation was assessed using a two-pulse protocol consisting of an initial step to −10 mV for 100 ms, a recovery interval of 2, 20, 200, or 1750 ms at −80 mV, and a test step to −10 mV. The current amplitude elicited by the test pulse was expressed as a fraction of the current from the initial step to give a measure of fractional recovery. The time course of recovery was fit with a Hill-Langmuir equation to accommodate apparent negative cooperativity in all of the datasets. $I = I_{max} \times X \exp(n)/(K \exp(n) + X \exp(n))$, where X = time (ms), and the cooperativity, n , was fixed at 0.31. Data were fit, and fits to datasets were compared using F-test in OriginPro 8.5.

RESULTS

In Conventional Recording Conditions the Splice Variants Show Similar Gating Behavior—Most heterologous expression studies of splice variants of neuronal sodium channels to date

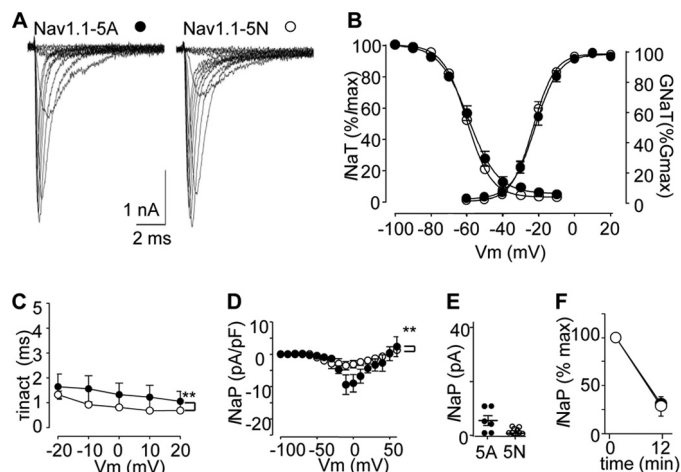


FIGURE 2. Kinetics- and voltage-dependent properties of Nav1.1 splice variants at room temperature using intracellular fluoride (CsF) solutions. *A*, splice variants produce similar overall currents. Raw traces from splice variants show currents elicited in response to a series of voltage steps when recorded with intracellular fluoride anions at room temperature. *B*, both splice variants have similar voltage dependence. Shown is an overlay of voltage dependence of activation and inactivation for Nav1.1-5A (filled symbols, $n = 9$ and 8) and Nav1.1-5N (open symbols, $n = 14$ and 12). Inactivation curves are percentages of peak transient currents (I_{NaT}) for each cell, and activation is shown as the percentage of peak transient conductances (G_{NaT}). *C*, shown is the rate of inactivation during steps to different potentials; symbols as in *B*. The Nav1.1-5N channels inactivated more rapidly in these conditions. The difference between the two sets of points is significant: **, $p \leq 0.01$; two-way ANOVA, Bonferroni post test (5A $n = 8$; 5N $n = 12$). *D*, shown is the percentage of current remaining 20 ms after steps to different potentials for both splice variants. In these conditions Nav1.1-5N channels (open symbols) have less non-inactivating currents (I_{NaP}) for steps near peak activation. The difference between the two sets of points is significant: **, $p \leq 0.01$; two-way ANOVA, Bonferroni post test (5A $n = 12$; 5N $n = 13$). *pF*, picofarads. *E*, shown is the absolute amplitude of persistent current from individual cells after ~12 min in whole cell configuration using intracellular solutions containing CsF. *F*, persistent or non-inactivating currents (I_{NaP}) run down during recordings. The percentage of I_{NaP} remaining after ~12 min of recording is shown for steps to −10 mV normalized to starting levels (0). Times are approximate to allow pooling of cells. Open symbols are 5N and filled symbols are 5A, but overlap obscures filled symbols. Error bars are S.E. (for time = 0; 5A $n = 12$; 5N $n = 13$; for time = 12; 5A $n = 6$; 5N $n = 9$).

have relied on intracellular fluoride to promote stable recordings (17, 20, 21, 24). We, therefore, started with similar recording conditions to compare Nav1.1 channels containing exon 5A (Nav1.1-5A) and 5N (Nav1.1-5N). In recordings with intracellular fluoride, the currents produced by both Nav1.1 splice variants exhibited the same voltage dependence of activation and inactivation (Fig. 2, *A* and *B*; Table 1). Nav1.1-5N channels, however, had a tendency to inactivate more rapidly, as indicated by a reduced time constant of inactivation (τ_{inact}) over a range of potentials (Fig. 2*C*). Between −20 and +20 mV they also underwent more complete inactivation during voltage steps, as indicated by a reduced non-inactivating or persistent current (I_{NaP}) 20 ms after the onset of the depolarizing step (Fig. 2, *D* and *E*). However, we noted that the amount of I_{NaP} decreased with the duration of the recording and after 12 min was largely absent (Fig. 2, *D* and *E*). This decrease of the I_{NaP} component was similar for Nav1.1-5A and Nav1.1-5N (Fig. 2*F*). In contrast, the peak transient current (I_{NaT}) did not change consistently, meaning that during a recording the percentage of current that inactivated during a voltage-step increased.

TABLE 1

Intrinsic parameters of currents from Nav1.1 splice variants

Values for CsF are not corrected for the difference in liquid junction potential compared to CsCl, which is consistent with the changes in V_{50} being due to the anions present in recording solutions. Data from CsF recordings are from >8 min after obtaining whole cell configuration (see "Experimental Materials"). All values are the mean \pm S.E. Although several parameters were significantly altered by recording conditions (see Figs. 5 and 6), none of the parameters reached significance when compared to the same condition against both of the other variants ($p > 0.05$ using 2-way ANOVA). V_{50} are in mV, and τ_{inact} was measured at -10 mV.

Variant of Na _v 1.1	Physiological temperature (CsCl)			Room temperature (CsF)			Room temperature (CsCl)		
	5A	5N	D207N	5A	5N	D207N	5A	5N	D207N
V_{50} act	-18.5 ± 0.9	-18.8 ± 0.8	-17.2 ± 1.3	-21.2 ± 1.7	-22.6 ± 1.2	-21.5 ± 0.6	-15.4 ± 1.1	-17.3 ± 1.3	-13.8 ± 1.1
k	6.7 ± 0.4	6.5 ± 0.3	6.3 ± 0.3	6.0 ± 0.4	5.4 ± 0.2	7.4 ± 0.5	6.2 ± 0.4	5.8 ± 0.4	6.1 ± 0.3
n	15	18	8	9	14	9	18	13	11
V_{50} inact	-53.7 ± 1.2	-53.1 ± 1.3	-55.2 ± 1.4	-58.4 ± 1.4	-60.1 ± 0.7	-59.3 ± 0.7	-54.1 ± 1.6	-58.0 ± 2.0	-53.9 ± 1.1
k	6.3 ± 0.3	5.9 ± 0.7	8.4 ± 0.7	8.1 ± 0.9	6.7 ± 0.4	6.9 ± 0.6	6.2 ± 0.5	6.9 ± 0.3	8.8 ± 0.1
n	15	11	8	8	12	9	14	9	9
% I _{NaP}	8.6 ± 1.6	5.2 ± 1.1	5.2 ± 0.8	7.8 ± 1.7	3.6 ± 1.1	1.7 ± 0.6	12.8 ± 2.5	12.2 ± 1.7	10.6 ± 2.8
n	16	11	11	12	13	9	10	8	9
τ_{inact}	0.5 ± 0.1	0.6 ± 0.1	0.5 ± 0.1	1.6 ± 0.5	0.9 ± 0.1	0.6 ± 0.2	2.4 ± 0.3	3.3 ± 0.6	2.4 ± 0.4
n	8	10	13	8	12	9	14	9	10

Changing the Intracellular Anion Affects Channel Behavior— A possible explanation for the loss of I_{NaP} current during long recordings is that cesium fluoride from the patch pipette gradually disrupts a process that normally inhibits Nav1.1 inactivation. Fluoride ions might alter gating by disrupting G-protein signaling (29, 30), which has been shown to affect the proportion of I_{NaP} mediated by sodium channels. Previous studies investigating this phenomenon were carried out with intracellular solutions that did not include fluoride (25). Indeed, in the presence of trace amounts of aluminum (for instance from the borosilicate pipette glass), fluoride assembles to aluminum tetrafluoride, which binds to and disrupts G-protein signaling as well as phosphatases (30).

To determine whether the time-dependent changes in I_{NaP} current were due to the presence of fluoride in intracellular solutions, we carried out similar recordings with fluoride ions replaced by chloride (Fig. 3; Table 1). In these conditions, where only the intracellular anion was changed, both splice variants of Nav1.1 inactivated more slowly. The effects were more pronounced on Nav1.1–5N channels, such that they now inactivated significantly more slowly than Nav1.1–5A channels (Fig. 3C), opposite to the pattern observed using fluoride-based intracellular solutions (Fig. 2C). Moreover, in recordings with intracellular chloride, I_{NaP}, the non-inactivating current, was similar for both variants (Fig. 3, D and E) and was more stable during prolonged recordings (Fig. 3F). Overall, these data suggest that the presence of fluoride anions, possibly conjugated with aluminum from the electrodes, affect Nav1.1 inactivation with a more pronounced effect on the splice variant containing exon 5N.

We observed an additional shift in the voltage dependence of activation and inactivation, but this was accounted for by a 5-mV junction potential difference between CsCl- and CsF-based solutions (see "Experimental Procedures") and is, therefore, unlikely to reflect an intrinsic change in channel gating.

Raising the Temperature Accelerates Inactivation and Abolishes Persistent Currents Mediated by Both Variants— A hallmark of seizures related to mutations in *SCN1A*, indeed of many sodium channel mutations (4, 5, 31), is their sensitivity to temperature. Most published recordings of Nav channels have been carried out at room temperature. To investigate how changing temperature specifically altered channel gating, we

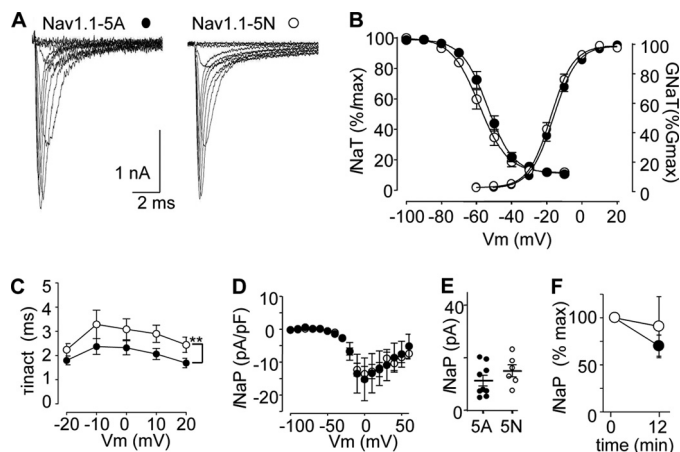


FIGURE 3. Substituting intracellular fluoride with chloride (CsCl) affects the rate and completeness of inactivation. *A*, sample traces from both splice variants show increased I_{NaP} currents in recordings at room temperature using intracellular chloride solution. *B*, the voltage dependence of activation and inactivation remains similar for both variants. The inactivation is incomplete, consistent with the increased proportion of I_{NaP}. Symbols and units are as in Fig. 2; filled = 5A ($n = 18$ activation, $n = 14$ inactivation); open = 5N, ($n = 13$ activation, $n = 9$ inactivation). *GNaT*, transient sodium conductance. *C*, the rate of inactivation is slowed by the replacement of intracellular fluoride with intracellular chloride (compare with Fig. 2C). The change is significant for Nav1.1–5N variants ($p < 0.0001$, two-way ANOVA, Bonferroni post test). With intracellular chloride, channels containing exon 5N inactivate more slowly than channels containing exon 5A, and the sets of data points are significantly different; **, $p \leq 0.01$; two-way ANOVA, Bonferroni's post test (5A $n = 14$; 5N $n = 9$). *D*, shown are increased I_{NaP} in recordings with intracellular chloride (compare with Fig. 2D). Both variants show a larger proportion of I_{NaP} in response to steps to a range of potentials. Because substituting chloride for fluoride has a larger effect on channels containing 5N, the difference between splice variants is occluded (5A $n = 10$; 5N $n = 8$). *pF*, picofarads. *E*, the absolute amplitude of persistent current from individual cells after ~8 min in whole cell configuration using intracellular solutions containing CsCl is shown. Points indicate individual cells. Currents were similar at 12 min, but because of the less stable configuration using a CsCl-based intracellular solution, fewer cells survived than when using solutions containing CsF. *F*, with intracellular chloride the proportion of I_{NaP} is more stable. As in Fig. 2F, the percentage of I_{NaP} remaining after ~12 min of recording is shown for steps to -10 mV normalized to starting levels (time = 0). Times are approximate to allow pooling of cells. Open symbols are 5N, and filled symbols are 5A. Error bars are S.E. (for time = 0; 5A $n = 10$; 5N $n = 8$; for time = 12; 5A $n = 7$; 5N $n = 4$).

carried out recordings at physiological temperatures. In particular, we asked whether changing the temperature had different consequences for the two splice variants. We used conditions identical to those in Fig. 3, except that the recording temperature was in the physiological range (37 ± 2 °C; Fig. 4; Table 1).

Splicing Modifies Inactivation of Nav1.1 Channels

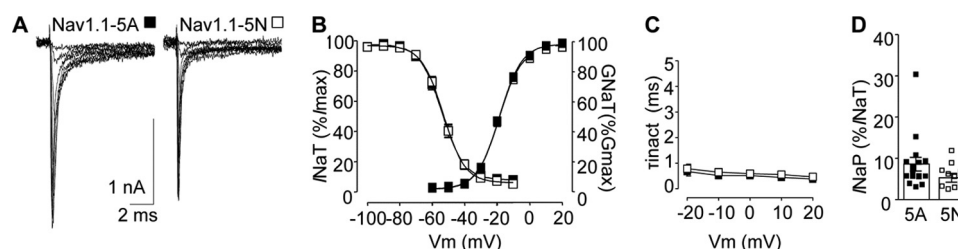


FIGURE 4. At physiological temperatures using intracellular chloride (CsCl) solutions, the splice variants mediate similar currents that inactivate rapidly and robustly. *A*, raw traces from both variants show the more rapid kinetics associated with higher temperatures. *B*, voltage dependence of activation and inactivation is largely unaffected by changing temperatures. *Filled symbols* = Nav1.1-5A ($n = 15$ activation; $n = 15$ inactivation), and *open symbols* = Nav1.1-5N ($n = 18$ activation, $n = 11$ inactivation); *error bars* are S.E. but are largely obscured by symbols. *G_{NaT}*, transient sodium conductance. *C*, the rate of inactivation is increased for both variants with very similar rates for each over a range of potentials (*filled*, 5A, $n = 16$, *open*, 5N, $n = 11$). *D*, the proportion of *I_{NaP}* is relatively small at higher temperatures. Cells are pooled from a time point ~2–5 min after obtaining whole cell configuration, and each symbol corresponds to an individual cell (5A, $n = 16$, 5N $n = 11$). It was not possible to measure the stability of these currents for prolonged recordings at physiological temperatures.

Recordings at supraphysiological temperatures (e.g. to mimic temperature changes during febrile seizures) were too unstable to allow robust comparison of the variants in these conditions (data not shown).

At physiological temperatures both variants inactivated more quickly, and the difference in τ_{inact} between Nav1.1-5N and Nav1.1-5A was occluded (Fig. 4C). Both variants also inactivated more completely than at room temperature, and the proportion of *I_{NaP}* was similar for both splice variants (Fig. 4D), consistent with recordings using CsF at room temperature.

At Physiological Temperatures β Subunits Do Not Distinguish between Splice Variants—We hypothesized that splice variants might associate differently with, or be differently modified by sodium channel β subunits. These transmembrane subunits are necessary for proper sodium channel signaling *in vivo*, as mutations in one of the β subunits are sufficient to cause epilepsy (32). *In vitro*, most work with β subunits has been carried out at room temperature, and the subunits have different effects depending on the conditions and cell lines used (33–35). We, therefore, co-expressed $\beta 1$ or its splice variant $\beta 1B$ with $\beta 2$ and each Nav1.1 variant using a tricistronic IRES vector (28) to ensure recorded cells were co-transfected with the β subunits and compared the gating at physiological temperatures using the CsCl-based intracellular solutions. In these conditions the β subunits had no consistent effects on voltage dependence of activation or inactivation (Table 2). The isoform $\beta 1B$, but not the $\beta 1$ isoform, slowed the rate of inactivation slightly for both variants (Table 2). We also noted that co-expression of $\beta 1B$ appeared to reduce the current density of both variants in these conditions but to a similar degree (data not shown). Thus, under our conditions, the β subunits had relatively modest effects on the channel gating and did not distinguish strongly between the two splice variants.

Modulation by G-proteins Is Suppressed at Physiological Temperatures—Our initial finding that inactivation was altered in the presence of intracellular fluoride anions is consistent with a role for G-protein signaling in regulating the inactivation of these channels. RT-PCR and array data indicated that our untransfected HEK cells express multiple G-protein subunits (data not shown). We used the nonspecific activator of G-proteins, GTP γ S, to ask whether activation of G-proteins played a role in modifying inactivation of the variants at higher temper-

atures. Recordings were carried out as in Fig. 4, but with 0.5 mM GTP γ S in the intracellular solution, as has previously been used to activate *I_{NaP}* in heterologously expressed Navs (36).

Activation of G-proteins under these conditions had no significant effects on the channels ($p > 0.05$; Table 2). These data are not consistent with earlier reports that activating G-proteins increases *I_{NaP}* currents mediated by Nav1.1 channels (only the 5A variant was explored) (25). However, those experiments were carried out at room temperature, so to confirm the effectiveness of our GTP γ S conditions we repeated the recordings at lower temperatures. Under these conditions constitutive activation of G-proteins with GTP γ S robustly increased *I_{NaP}*, consistent with the changes reported previously and with the 5N-containing channels slightly more altered than those containing 5A (data not shown).

Inactivation Kinetics Differ Consistently between the Splice Variants—Changing either temperature or the major intracellular anion had more pronounced effects on the inactivation of 5N-containing channels with respect both to the rate of inactivation (τ_{inact} ; Fig. 5A) and the proportion of non-inactivating currents, *I_{NaP}* (Fig. 5B). In the case of *I_{NaP}*, only 5N-containing channels were significantly affected. These data suggest that the presence of exon 5N may have specific effects on the stability of inactivation, with the 5N channels more sensitive to intracellular anions (possibly via G-proteins) and temperature.

Because 5N-containing channels appeared to be more sensitive to recording conditions both with respect to the rate and completeness of inactivation, we examined a further parameter describing the inactivation kinetics of these channels. We asked whether the 5N-containing channels had different rates of recovery from inactivation compared with 5A by constructing a time-course of recovery from inactivation. At physiological temperatures it was not possible to maintain individual cells throughout the entire recovery protocol, and consequently data from multiple cells were combined to obtain full datasets for each variant.

Nav1.1 channels containing exon 5N recovered more rapidly from inactivation than those containing 5A (Fig. 5C). This was illustrated by significantly more channels being available at 2 ms ($p = 0.03$, two-tailed *t* test). In addition, the recovery time-course at 37 °C was also significantly different ($p = 0.0011$; F-test) when fit with a Hill-Langmuir equation (see Table 3).

TABLE 2

Parameters of currents from Nav1.1 splice variants in the presence of β subunits and GTP γ S

All recordings were carried out at physiological temperatures using CsCl-based intracellular. V_{50} values are in mV, and τ_{inact} was measured at -10 mV. Data in the first two columns are repeated from Table 1 for convenience. All values are the mean \pm S.E. None of the parameters reached significance when compared against the other conditions ($p > 0.05$ using 2-way ANOVA).

Variant of Na _v 1.1	With β subunits				With β 1B subunits		With GTP γ S	
	5A	5N	5A β 1 β 2	5N β 1 β 2	5A β 1B β 2	5N β 1B β 2	5A	5N
V_{50} act	-18.5 ± 0.9	-18.8 ± 0.8	-19.3 ± 1.5	-20.6 ± 1.0	-15.7 ± 3.2	-20.3 ± 2.9	-18.3 ± 1.3	-21.6 ± 8.4
K	6.7 ± 0.4	6.5 ± 0.3	$6.6 \pm .04$	5.6 ± 0.6	7.4 ± 0.7	7.5 ± 0.6	5.7 ± 2.6	5.5 ± 0.4
n	15	18	12	7	7	10	12	13
V_{50} inact	-53.7 ± 1.2	-53.1 ± 1.3	-55.9 ± 1.3	-57.2 ± 1.9	-57.5 ± 0.8	-56.8 ± 0.7	-53.6 ± 1.9	-56.3 ± 0.9
k	6.3 ± 0.3	5.9 ± 0.7	7.2 ± 0.3	7.0 ± 0.6	7.4 ± 1.3	6.9 ± 0.6	5.7 ± 0.8	5.5 ± 0.2
n	15	11	8	8	3	4	9	14
% INaP	8.6 ± 1.6	5.2 ± 1.1	7.9 ± 1.2	6.6 ± 1.6	9.5 ± 5.2	7.1 ± 2.5	4.6 ± 0.9	3.6 ± 0.5
n	16	11	8	8	3	4	9	14
τ_{inact}	0.5 ± 0.1	0.6 ± 0.1	0.8 ± 0.2	0.8 ± 0.2	0.8 ± 0.2	0.8 ± 0.2	0.3 ± 0.0	0.3 ± 0.0
N	8	10	8	8	7	11	11	12

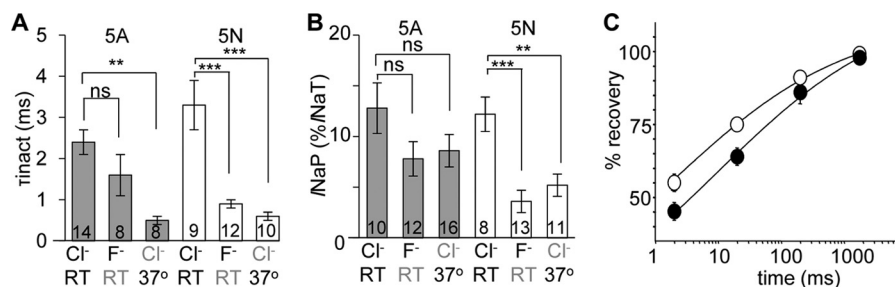


FIGURE 5. Nav1.1–5N channels show larger temperature- and anion-dependent changes in rate and completeness of inactivation and recover more quickly from inactivation. *A*, although the rate of inactivation is significantly increased for both variants, the change is larger and more significant for those containing exon 5N. Numbers indicate the number of cells measured in each condition. RT, room temperature. *B*, the proportion of INaP shows a trend toward a reduction for channels containing exon 5A, but for channels containing 5N, this reduction is robust and significant. **, $p < 0.01$; ***, $p < 0.001$; ns, $p > 0.05$; 2-way ANOVA, Tukey's post hoc test for multiple comparisons. Numbers indicate the number of cells measured in each condition. *C*, recovery from inactivation is faster for channels containing exon 5N (open symbols, $n = 6$ –10) than for channels containing exon 5A (filled symbols, $n = 6$ –8). The fits are significantly different ($P(5N = 5A) = 0.0011$; F-test).

TABLE 3

Parameters and quality of non-linear curve fitting of recovery from inactivation

All fits were to recordings carried out at physiological temperatures using CsCl-based intracellular. To improve the accuracy of the fit, the cooperativity was fixed at 0.31 (negative cooperativity) for all three datasets. K is in mV. S.E. is the error of the fit. R-squared indicates the coefficient of determination. 5–13 cells were recorded for each variant at each time point. Because of the reduced stability of recordings at physiological temperatures, not all time points are from the same cells.

Variant of Na _v 1.1	5A	5N	D207N
$I_{\text{max}} \pm$ S.E.	1.18 ± 0.02	1.11 ± 0.01	1.16 ± 0.01
$K \pm$ S.E.	9.86 ± 1.70	1.85 ± 0.26	3.56 ± 0.36
R^2	0.998	0.998	0.999

The Change in Recovery from Inactivation Is Accounted for by a Single Amino Acid Change Introduced by Splicing—As mentioned above, the channels encoded by Nav1.1–5A and Nav1.1–5N differ by three amino acids (Fig. 1A). It is possible that the difference in stability of inactivation arises from all three amino acids or from the two phenylalanines that are specific to human Nav1.1–5N. To test these possibilities we constructed a clone that differed from Nav1.1–5A only at the conserved aspartate to asparagine site (Nav1.1–D207N). This change is conserved in the extracellular S3–S4 linkers encoded by alternate exons in tetrodotoxin-sensitive neuronal sodium channels (Fig. 1A).

At physiological temperatures Nav1.1–D207N channels had similar voltage dependence, rate, and completeness of inactivation as both splice variants (Fig. 6, A–C; Table 1). However, as with Nav1.1–5N, changing the intracellular solution to one

based on CsF had significant effects on the rate of inactivation and on the proportion of INaP (Fig. 6, D and E). Increasing the temperature also robustly altered the rate of inactivation (Fig. 6D) and had a tendency to reduce INaP, which did not reach significance ($p > 0.05$; 2-way ANOVA).

Moreover, the recovery from inactivation for D207N channels was similar to Nav1.1–5N channels ($p > 0.05$; F-test with Bonferroni correction) and significantly faster than Nav1.1–5A channels ($p = 0.002$; F-test with Bonferroni correction; Fig. 6F). These data suggest that the change in recovery from inactivation between the splice variants can be reproduced by the single amino acid change of D207N and that the two phenylalanines introduced by splicing do not have significant effects on this parameter.

We further explored the role for residue 207 in the S3–S4 linker in modifying the sensitivity of the inactivation to CsF using a serendipitous mutation in an Nav1.1–5N clone that changed Asp-207 to a histidine (D207H, in the 5N background with two phenylalanines). The D207H mutant generated channels that produced large persistent currents in room temperature in recordings with CsCl-based intracellular solution (INaP = $29 \pm 3\%$ of transient currents; $n = 10$). This proportion of INaP was significantly larger than both Nav1.1–5N and the D207N channels ($p < 0.001$ for both, one way ANOVA, with Tukey–Kramer post test). However, similar to the Nav1.1–5N and the D207N channels, these persistent currents were completely suppressed when recording at room temperature with

Splicing Modifies Inactivation of Nav1.1 Channels

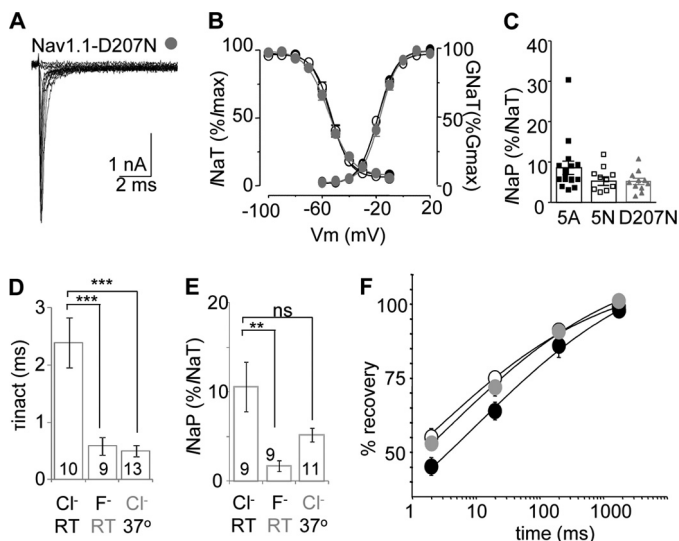


FIGURE 6. The conserved D207N change produces channels similar to 5A and 5N at physiological temperatures using chloride based intracellular solutions (CsCl). A, shown are sample traces from channels containing the D207N change but otherwise identical to Nav1.1-5A. B, voltage dependence of activation and inactivation are similar for D207N channels (gray symbols; activation $n = 8$, inactivation $n = 8$). Data from Fig. 5 are included for comparison. G_{NaT} , transient sodium conductance. C, D207N channels produce similar amounts of non-inactivating currents to 5N channels. D–E, as with channels containing exon 5N, D207N channel inactivation is sensitive to the presence of fluoride with both the rate (D) and amount (E) of inactivation (as indicated by proportion of I_{NaP}) and was significantly reduced in recordings containing this intracellular anion. Temperature also significantly increased the rate of inactivation (D). However, although D207N channels at increased temperatures had a tendency to produce less I_{NaP} , the variability of this parameter in cells at room temperature (RT) meant the change failed to reach significance. Numbers in the columns indicate the number of cells sampled in each condition. F, recovery from inactivation for D207N channels (gray, $n = 5$ –13) is similar to 5N channels (open, $P(\text{D207N} = 5N) > 0.05$; F-test with Bonferroni correction) and significantly faster than 5A channels (black, $P(\text{D207N} = 5A) = 0.002$; F-test with Bonferroni correction). Data from Fig. 5 are included for comparison. **, $p < 0.01$; ***, $p < 0.001$; ns, $p > 0.05$; 2-way ANOVA, Tukey's post hoc test for multiple comparisons.

CsF-based intracellular solutions ($-1 \pm 3\%$ $n = 5$; $p < 0.0001$; two tailed t test). Note that, in contrast, intracellular fluoride did not significantly reduce I_{NaP} in channels with the 5A sequence (Fig. 5A). These data indicate that the Asp-207 site in the S3-S4 linker of domain I is involved in setting the stability of inactivation of these channels and underline the importance of this site in modulating inactivation.

DISCUSSION

We have shown that alternative splicing in human Nav1.1 channels modifies inactivation of the channels. In particular, both the naturally occurring alternate exon 5N with three amino acid changes and an artificial variant containing only the conserved aspartate to asparagine change (D207N) recover from inactivation more rapidly than channels containing the sequence encoded by exon 5A.

The altered stability of inactivation may be related to the finding that manipulating recording conditions (ionic composition or temperature) consistently had more robust effects on 5N-containing channels than on those containing 5A. However, variability among cells, particularly in the proportion of persistent current, prevents direct comparison of the change induced in each condition.

The impact of splicing on inactivation is potentially important for the role of this channel in human epilepsies. Several mutations that alter either the amount of, or recovery from, inactivation have been associated with monogenetic epilepsy in human kindreds (5, 26). Single channel analysis indicates that these mutations can have specific effects on inactivation (37), and mouse models carrying mutant channels have altered recovery from inactivation in interneurons (7, 9). In addition, a polymorphism that reduces the amount of exon 5N in human *SCN1A* mRNA has been associated with an altered dosage of drugs that are used to treat epilepsy (10–12) and possibly with an altered likelihood of developing some types of seizures (14, 15) (but see Refs. 13 and 16). Our data suggest that inactivation is specifically modified by splicing, and this parameter may contribute to different drug sensitivities or seizure likelihoods, although further studies are needed to determine how strong a relationship exists or whether splicing modifies the severity of mutations or other variants found in *SCN1A*.

The rate of recovery of sodium channels from inactivation is implicated in the mechanism of action of several frontline anti-epileptic drugs including phenytoin, carbamazepine, and lamotrigine. The dosage and/or serum levels of these drugs have been reported to vary with the polymorphism that modifies splicing at this site in human *SCN1A* (10–12). These drugs exert use-dependent effects on sodium channels by selectively binding to and stabilizing the inactive states (38, 39). The reduction in the rate of recovery from inactivation may underlie their effectiveness in epilepsy. This raises the question of whether alternative splicing, by including exon 5N and consequently increasing the rate of recovery from inactivation, also increases the likelihood of seizures. However, any hypothetical mechanism is complicated by the diversity of neuronal types and the observation that Nav1.1 channels (both splice variants) are expressed by inhibitory interneurons. Indeed, changes in splicing of *SCN1A*/Nav1.1 might have disproportionate effects on interneurons (7–9), whereas the up-regulated splicing in other voltage-gated channels could have counter effects in excitatory neurons (40, 41). These potentially opposite influences on circuit excitability make it difficult to predict the overall impact of splicing on seizures.

Because the site of the D207N substitution is in the short S3-S4 linker adjacent to a charged S4 voltage-sensor, a straightforward hypothesis would be that by toggling a charged residue in and out of this linker, alternative splicing might modify voltage dependence of activation. However, we did not see consistent differences in voltage dependence of either activation or inactivation. Instead the results of this study imply that, despite its predicted external location, the S3-S4 linker plays a role in modulating inactivation. This observation is consistent with an early report showing that the S3-S4 linker in the fourth domain can also play a role in regulating the rate of recovery from inactivation (42). A conserved splicing event, which among other changes introduces two negatively charged aspartates at the congruous position in the third domain (eight amino acids before the first arginine of the S4), has recently been shown to play a role in setting the amount of I_{NaP} carried by *Drosophila* Nav channels (22). However, with the additional changes in that splicing it is not possible to determine whether the intro-

duction of a negative charge at the position equivalent to Asp-207 in DI of Nav1.1 is sufficient to alter I_{NaP} .

The impact on inactivation of an amino acid, which is predicted to be relatively superficial in the channel structure, suggests a role for the position of the voltage-sensing module in the first domain in modulating the affinity of the inactivation particle for the intracellular surface of this channel, possibly by altering the positions of the S3 or S4 intracellular regions. The recent structure of sodium channels (43) is thought to represent the extruded S4 position, linked to a still closed channel pore (a pre-open state). In that structure the shape of the S3-S4 linker is noted to be poorly defined, consistent with high mobility (43). Our data indicate that altering this linker may induce an allosteric change to the intracellular surface of the channel that leads to altered affinity for the inactivation particle.

These data potentially bring together some of the disparate data from different sodium channels that are alternatively spliced at this site and point to inactivation as a candidate target of this conserved site of alternative splicing. Room temperature recordings in the absence of fluoride from the more distantly related cardiac sodium channel (Nav1.5) splice variants indicated that the 5N version of the channel inactivated more slowly than the 5A version (23). This is similar to our findings in the room temperature recordings from variants of Nav1.1 (Fig. 3), although the sequences of exon 5N are divergent. Nav1.7 channels containing exons 5N and 5A have a slightly different development of inactivation in room temperature recordings using cesium fluoride-based intracellular solutions; however, these conditions did not reveal a difference in recovery from inactivation for variants of Nav1.7 (17). Finally, a study also using cesium fluoride in the intracellular solutions showed an increased level of persistent current from the closely related neuronal Nav1.2 channels containing exon 6N (corresponding to 5N in Nav1.1) (21), which is similar to the changes seen in Nav1.1 in similar conditions (Fig. 2). By using three different recording conditions in one study, we show that the different changes reported for splice variants from different Nav1s may reflect the recording conditions used.

The finding that intracellular fluoride has robust effects on persistent currents mediated by Nav1.1 is consistent with a study showing a similar effect on Nav1.6 channels expressed in HEK cells (44). It remains to be determined whether this anion sensitivity is also exhibited by other sodium channels. Nevertheless, these results clearly call for caution in extrapolating observations made with fluoride to more physiological situations.

Although it is clear that β subunits are necessary for Nav1.1 function *in vivo*, the role of these subunits *in vitro* may depend on the recording conditions. We used tricistronic vectors (28) to ensure that cells we recorded had been co-transfected with the β subunit construct; however, it is possible that expression from this vector was low or that at physiological temperatures in HEK cells the β subunits are not trafficked successfully. The lack of consistent effects of β subunits in recordings at physiological temperatures is most likely due to the non-neuronal expression system; HEK cells may not share intracellular anchoring proteins that interact with β subunits in neurons and are not be able to replicate some of the functional effects of β

subunits (32). We did not investigate the effects of all permutations of β subunits, and it is possible that other combinations, such as those with $\beta 4$, which have been shown to modify persistent currents (45), could have variant-specific effects in HEK cells.

We focused on the splice variants of $\beta 1$ subunits because these are most closely associated with Nav1.1, particularly with regard to clinical manifestation, where mutations in either SCN1A or SCN1B can give rise to the same epilepsy syndrome, GEFS+ (generalized epilepsy with febrile seizures plus) (32). However, it is important to note that the regulation of splicing in SCN1A may mean that $\beta 1$ subunits are relatively less likely to co-exist with Nav1.1-5N channels. The neonatal splice variant is more prevalent early in development where not all sodium channels are bound to β subunits (46). In addition, $\beta 1$ subunits appear to be down-regulated in epilepsy (47), when exon 5N is up-regulated in several sodium channels (40, 41), further implying that these subunits may have complementary expression patterns to the neonatal splice variants.

Finally, the modulation of persistent currents depends steeply on temperature. Although our data confirm that G-proteins can modify sodium currents mediated by Nav1.1 channels (25) and suggest this modulation may be more pronounced for splice variants containing exon 5N, exploring the significance of this modulation or of modulation by β subunits in neurons is not trivial because the rodent *SCN1A* gene does not contain a functional copy of exon 5N, and any variant-specific effects will, therefore, be lost. In summary, alternative splicing affects the rate at which Nav1.1 channels recover from inactivation, and this change is due to a conserved amino acid change that may exert similar effects on several neuronal sodium channels in physiological conditions.

Acknowledgments—We thank M. Mantegazza and H. Lerche for generously sharing human Nav1.1 cDNAs.

REFERENCES

- Copley, R. R. (2004) *Trends Genet.* **20**, 171–176
- Gazina, E. V., Richards, K. L., Mokhtar, M. B., Thomas, E. A., Reid, C. A., and Petrou, S. (2010) *Neuroscience* **166**, 195–200
- Bean, B. P. (2007) *Nat. Rev. Neurosci.* **8**, 451–465
- Catterall, W. A., Kalume, F., and Oakley, J. C. (2010) *J. Physiol.* **588**, 1849–1859
- Escayg, A., and Goldin, A. L. (2010) *Epilepsia* **51**, 1650–1658
- Mantegazza, M., Rusconi, R., Scalmani, P., Avanzini, G., and Franceschetti, S. (2010) *Epilepsy Res.* **92**, 1–29
- Tang, B., Dutt, K., Papale, L., Rusconi, R., Shankar, A., Hunter, J., Tufik, S., Yu, F. H., Catterall, W. A., Mantegazza, M., Goldin, A. L., and Escayg, A. (2009) *Neurobiol. Dis.* **35**, 91–102
- Yu, F. H., Mantegazza, M., Westenbroek, R. E., Robbins, C. A., Kalume, F., Burton, K. A., Spain, W. J., McKnight, G. S., Scheuer, T., and Catterall, W. A. (2006) *Nat. Neurosci.* **9**, 1142–1149
- Martin, M. S., Dutt, K., Papale, L. A., Dubé, C. M., Dutton, S. B., de Haan, G., Shankar, A., Tufik, S., Meisler, M. H., Baram, T. Z., Goldin, A. L., and Escayg, A. (2010) *J. Biol. Chem.* **285**, 9823–9834
- Heinzen, E. L., Yoon, W., Tate, S. K., Sen, A., Wood, N. W., Sisodiya, S. M., and Goldstein, D. B. (2007) *Am. J. Hum. Genet.* **80**, 876–883
- Tate, S. K., Depondt, C., Sisodiya, S. M., Cavalleri, G. L., Schorge, S., Soranzo, N., Thom, M., Sen, A., Shorvon, S. D., Sander, J. W., Wood, N. W., and Goldstein, D. B. (2005) *Proc. Natl. Acad. Sci. U.S.A.* **102**, 5507–5512

Splicing Modifies Inactivation of Nav1.1 Channels

12. Tate, S. K., Singh, R., Hung, C. C., Tai, J. J., Depondt, C., Cavalleri, G. L., Sisodiya, S. M., Goldstein, D. B., and Liou, H. H. (2006) *Pharmacogenet. Genomics* **16**, 721–726
13. Zimprich, F., Stogmann, E., Bonelli, S., Baumgartner, C., Mueller, J. C., Meitinger, T., Zimprich, A., and Strom, T. M. (2008) *Epilepsia* **49**, 1108–1109
14. Abe, T., Seo, T., Ishitsu, T., Nakagawa, T., Hori, M., and Nakagawa, K. (2008) *Br. J. Clin. Pharmacol.* **66**, 304–307
15. Schlachter, K., Gruber-Sedlmayr, U., Stogmann, E., Lausecker, M., Hotzy, C., Balzar, J., Schuh, E., Baumgartner, C., Mueller, J. C., Illig, T., Wichmann, H. E., Lichtner, P., Meitinger, T., Strom, T. M., Zimprich, A., and Zimprich, F. (2009) *Neurology* **72**, 974–978
16. Petrovski, S., Scheffer, I. E., Sisodiya, S. M., O'Brien, T. J., and Berkovic, S. F. (2009) *Neurology* **73**, 1928–1930
17. Chatelier, A., Dahllund, L., Eriksson, A., Krupp, J., and Chahine, M. (2008) *J. Neurophysiol.* **99**, 2241–2250
18. Chioni, A. M., Fraser, S. P., Pani, F., Foran, P., Wilkin, G. P., Diss, J. K., and Djamgoz, M. B. (2005) *J. Neurosci. Methods* **147**, 88–98
19. Choi, J. S., Cheng, X., Foster, E., Leffler, A., Tyrrell, L., Te Morsche, R. H., Eastman, E. M., Jansen, H. J., Huehne, K., Nau, C., Dib-Hajj, S. D., Drenth, J. P., and Waxman, S. G. (2010) *Brain* **133**, 1823–1835
20. Jarecki, B. W., Sheets, P. L., Xiao, Y., Jackson, J. O., 2nd, and Cummins, T. R. (2009) *Channels* **3**, 259–267
21. Liao, Y., Deprez, L., Maljevic, S., Pitsch, J., Claes, L., Hristova, D., Jordanova, A., Ala-Mello, S., Bellan-Koch, A., Blazevic, D., Schubert, S., Thomas, E. A., Petrou, S., Becker, A. J., De Jonghe, P., and Lerche, H. (2010) *Brain* **133**, 1403–1414
22. Lin, W. H., Wright, D. E., Muraro, N. I., and Baines, R. A. (2009) *J. Neurophysiol.* **102**, 1994–2006
23. Onkal, R., Mattis, J. H., Fraser, S. P., Diss, J. K., Shao, D., Okuse, K., and Djamgoz, M. B. (2008) *J. Cell Physiol.* **216**, 716–726
24. Xu, R., Thomas, E. A., Jenkins, M., Gazina, E. V., Chiu, C., Heron, S. E., Mulley, J. C., Scheffer, I. E., Berkovic, S. F., and Petrou, S. (2007) *Mol. Cell. Neurosci.* **35**, 292–301
25. Mantegazza, M., Yu, F. H., Powell, A. J., Clare, J. J., Catterall, W. A., and Scheuer, T. (2005) *J. Neurosci.* **25**, 3341–3349
26. Lossin, C. (2009) *Brain Dev.* **31**, 114–130
27. Schaller, K. L., Krzemien, D. M., McKenna, N. M., and Caldwell, J. H. (1992) *J. Neurosci.* **12**, 1370–1381
28. Cox, J. J., Reimann, F., Nicholas, A. K., Thornton, G., Roberts, E., Springell, K., Karbani, G., Jafri, H., Mannan, J., Raashid, Y., Al-Gazali, L., Hamamy, H., Valente, E. M., Gorman, S., Williams, R., McHale, D. P., Wood, J. N., Gribble, F. M., and Woods, C. G. (2006) *Nature* **444**, 894–898
29. Bigay, J., Deterre, P., Pfister, C., and Chabre, M. (1985) *FEBS Lett.* **191**, 181–185
30. Strunecká, A., Strunecký, O., and Patocka, J. (2002) *Physiol. Res.* **51**, 557–564
31. Schorge, S., Ptáček, L. J., and Páček, L. J. (2006) *Neurology* **67**, 1538–1539
32. Patino, G. A., and Isom, L. L. (2010) *Neurosci. Lett.* **486**, 53–59
33. Isom, L. L., Scheuer, T., Brownstein, A. B., Ragsdale, D. S., Murphy, B. J., and Catterall, W. A. (1995) *J. Biol. Chem.* **270**, 3306–3312
34. Meadows, L. S., Chen, Y. H., Powell, A. J., Clare, J. J., and Ragsdale, D. S. (2002) *Neuroscience* **114**, 745–753
35. Qu, Y., Curtis, R., Lawson, D., Gilbride, K., Ge, P., DiStefano, P. S., Silos-Santiago, I., Catterall, W. A., and Scheuer, T. (2001) *Mol. Cell. Neurosci.* **18**, 570–580
36. Ma, J. Y., Catterall, W. A., and Scheuer, T. (1997) *Neuron* **19**, 443–452
37. The, Y. K., Fernandes, J., Popa, M. O., Alekov, A. K., Timmer, J., and Lerche, H. (2006) *Biophys. J.* **90**, 3511–3522
38. Czapiński, P., Blaszczyk, B., and Czuczwar, S. J. (2005) *Curr. Top. Med. Chem.* **5**, 3–14
39. Rogawski, M. A., and Löscher, W. (2004) *Nat. Rev. Neurosci.* **5**, 553–564
40. Aronica, E., Yankaya, B., Troost, D., van Vliet, E. A., Lopes da Silva, F. H., and Gorter, J. A. (2001) *Eur. J. Neurosci.* **13**, 1261–1266
41. Gastaldi, M., Bartolomei, F., Massacrier, A., Planells, R., Robaglia-Schlupp, A., and Cau, P. (1997) *Brain Res. Mol. Brain Res.* **44**, 179–190
42. Dib-Hajj, S. D., Ishikawa, K., Cummins, T. R., and Waxman, S. G. (1997) *FEBS Lett.* **416**, 11–14
43. Payandeh, J., Scheuer, T., Zheng, N., and Catterall, W. A. (2011) *Nature* **475**, 353–358
44. Burbidge, S. A., Dale, T. J., Powell, A. J., Whitaker, W. R., Xie, X. M., Romanos, M. A., and Clare, J. J. (2002) *Brain Res. Mol. Brain Res.* **103**, 80–90
45. Aman, T. K., Grieco-Calub, T. M., Chen, C., Rusconi, R., Slat, E. A., Isom, L. L., and Raman, I. M. (2009) *J. Neurosci.* **29**, 2027–2042
46. Scheinman, R. I., Auld, V. J., Goldin, A. L., Davidson, N., Dunn, R. J., and Catterall, W. A. (1989) *J. Biol. Chem.* **264**, 10660–10666
47. Ellerkmann, R. K., Remy, S., Chen, J., Sochivko, D., Elger, C. E., Urban, B. W., Becker, A., and Beck, H. (2003) *Neuroscience* **119**, 323–333